ORIGINAL ARTICLE

Basic Study

Time-dependent impact of a high-fat diet on the intestinal barrier of male mice

Carolline Santos Miranda, Daiana Araujo Santana-Oliveira, Isabela Lopes Vasques-Monteiro, Nathan Soares Dantas-Miranda, Jade Sancha de Oliveira Glauser, Flavia Maria Silva-Veiga, Vanessa Souza-Mello

Carolline Santos Miranda, Daiana Araujo Santana-Oliveira, Isabela Lopes Vasques-Monteiro, Nathan Soares Dantas-Miranda, Jade Sancha de Oliveira Glauser, Flavia Maria Silva-Veiga, Vanessa Souza-Mello, Department of Anatomy, Rio de Janeiro State University, Rio de Janeiro 20551030, Brazil

Corresponding author: Vanessa Souza-Mello, PhD, Associate Professor, Department of Anatomy, Rio de Janeiro State University, Blvd. 28 de setembro 87, fundos, Rio de Janeiro 20551030, Brazil. souzamello.uerj@gmail.com

Abstract

BACKGROUND
Excessive saturated fat intake compromises the integrity of the intestinal mucosa, leading to low-grade inflammation, impaired mucosal integrity, and increased intestinal permeability, resulting in the migration of lipopolysaccharide (LPS) to other tissues.

AIM
To evaluate the chronic effects (at 10 and 16 wk) of a high-fat diet (HFD) (with 50% energy as fat) on the phylogenetic gut microbiota distribution and intestinal barrier structure and protection in C57BL/6 mice.

METHODS
Forty adult male mice were divided into four nutritional groups, where the letters refer to the type of diet (control and HFD or HF) and the numbers refer to the period (in weeks) of diet administration: Control diet for 10 wk, HFD for 10 wk, control diet for 16 wk, and HFD for 16 wk. After sacrifice, biochemical, molecular, and stereological analyses were performed.

RESULTS
The HF groups were overweight, had gut dysbiosis, had a progressive decrease in occludin immunostaining, and had increased LPS concentrations. Dietary progression reduced the number of goblet cells per large intestine area and *Mucin2* expression in the HF16 group, consistent with a completely disarranged intestinal ultrastructure after 16 wk of HFD intake.

CONCLUSION
Chronic HFD intake causes overweight, gut dysbiosis, and morphological and

functional alterations of the intestinal barrier after 10 or 16 wk. Time-dependent reductions in goblet cell numerical density and mucus production have emerged as targets for countering obesity-driven intestinal damage.

Core Tip: There is great interest in the scientific community in the impact of unhealthy eating habits, such as excess saturated fatty acid intake, on the gut microbiota composition and metabolic disease onset. Here, we evaluated the progressive changes in the intestinal structural barrier and gut microbiota composition in mice fed a high-fat diet (HFD) for 10 or 16 wk. HFD administration resulted in gut dysbiosis, compensatory enhancement of goblet cell numerical density, and increased *Mucin2* expression after 10 wk. Continuous feeding reduced the goblet cell number and the expression of *Mucin2* and occludin, consistent with the impaired tight junction ultrastructure in the chronically obese HFD-fed mice after 16 wk.

INTRODUCTION

Obesity is an undeniable health challenge worldwide due to its increasing prevalence in recent decades. Although it is a multifactorial disease, a positive energy balance is a frequent trigger. Excessive accumulation or abnormal body fat distribution results in a state of low-grade chronic inflammation, which is a potential risk factor for many metabolic disorders, including oral glucose intolerance, insulin resistance, dyslipidemia, metabolic-associated fatty liver disease, and type 2 diabetes[1,2].

Recent evidence suggests that the gut barrier should be a new study target for understanding the obesity epidemic[3, 4]. A high-fat diet (HFD) increases plasma lipopolysaccharide (LPS) concentrations by 2 to 3 times compared to a control diet[5]. Intestinal LPS can impair gut barrier integrity, leading to the leakage of LPS into the systemic circulation, inducing chronic inflammation, and contributing to metabolic endotoxemia and obesity[6].

The intestinal epithelial barrier regulates absorption, secretion, and protection to prevent systemic entry of antigens from the intestinal lumen[7,8]. Tight junctions (TJs), located in the apical portion of the lateral membrane of intestinal epithelial cells (IECs), are composed of multiple proteins, including the transmembrane protein occludin, that regulate intestinal permeability. Nutritional factors, such as irregular consumption of protein and casein peptides[3], may alter the dynamic regulation of intracellular occludin in TJs, specifically the permeability barrier to macromolecules[9]. A leaky gut facilitates the translocation of potentially harmful antigens into epithelial cells[10].

A hydrated gel composed of mucins secreted by goblet cells covers the luminal surface of the intestinal mucosa[11]. In an intact epithelium, this surface restricts the passage of most hydrophilic solutes[12]. However, studies on the effects of an HFD on gut barrier structure are contradictory. A previous study reported that HFD intake resulted in an increased number of goblet cells[13]. However, other studies have shown a significant reduction in goblet cell numerical density in HFD-fed mice[1,14]. These inconsistent results may be due to differences in the duration of HFD consumption and the age of the mice.

The present study hypothesized that HFD feeding elicits time-dependent changes in the gut microbiota composition, intestinal barrier structure, and protection. The majority of the mouse models were subjected to diet-induced obesity protocols (10 wk) or posttreatment (16 wk).

MATERIALS AND METHODS

Animals and ethics approval

All procedures performed in the present study complied with the Arrive Guidelines. The procedures followed the National Institutes of Health Guide for the Care and Use of Laboratory Animals and Brazilian Federal Law No. 11.794/ 2008, in addition to adhering to European Union standards on animals used for scientific purposes protection. The local Ethics Committee (Institute of Biology, CEUA N° 017/2021) approved the experimental design.

Twenty adult male C57BL/6 mice were housed in cages (5 rats per cage). The cages were maintained at a controlled temperature (21 ± 2 °C) and humidity (60% ± 10%), and the mice had free access to water and food. The cages allowed for sufficient ventilation and were arranged on a rack (NexGen Mouse 500, Allentown, PA, United States). The environment included light-dark cycles of 12/12 h and air renewal (15 min/h).

The sample size was considered the minimum needed to reach statistical significance based on the Ethics Committee recommendation. There was no animal exclusion during the experiment. The first author was aware of each group allocation, and procedures were first applied to the control group.

Experimental design

Twenty adult mice (3 months old) were included in this study. Initially, the animals were randomly assigned to one of the two nutritional groups: (1) The control group (C) (*n* = 10) was fed a control diet (14% of the total energy was protein, 10% was fat, and 76% was carbohydrate; the total energy was 15 KJ/g); and (2) The HF (*n* = 10) group was fed an HFD (14% of the total energy was protein, 50% was fat, and 36% was carbohydrate; the total energy was 21 KJ/g).

After 10 wk, five animals from each group were sacrificed. The other five animals in each group were fed the same diet for 16 wk, resulting in four study groups (*n* = 5 per group): Animals fed the C diet for 10 wk (C10), animals fed the HFD for 10 wk (HF10), animals fed the C diet for 16 wk (C16), and animals fed the HFD for 16 wk (HF16). PragSoluções (www.pragsolucoes.com.br, Jaú, São Paulo, Brazil) produced the experimental diets according to the recommendations of the American Institute of Nutrition (AIN 93M)[15].

Sample preparation

Mice were fasted for 6 h and sacrificed under anesthesia with ketamine (240 mg/kg) and xylazine (30 mg/kg). Blood samples were harvested by cardiac puncture, and plasma was obtained through centrifugation (712 × *g*) for 15 min and frozen (-80 °C) for further analysis. The small and large intestines were carefully dissected, weighed, and fixed in Millonig formalin for microscopic analysis or frozen at -80 °C for molecular analysis.

Plasma analysis

Plasma concentrations of LPS (multispecies LPS ELISA Kit Cat #SEB526Ge-96T; Cloud-Clone Corp., Katy, United States) were analyzed in duplicate with commercially available ELISA kits using Fluostar Omega equipment (BMG LABTECH GmbH, Germany).

Histology and stereology

After dissection, the large intestines (cecum) of the animals were fixed in Millonig for 48 h, followed by incubation in Paraplast Plus (Sigma-Aldrich Co., St. Louis, MO, United States). The tissues were cut into 5-μm-thick sections and subjected to alcian blue staining. Photomicrographs were obtained with a Lumenera camera and Olympus BX51 microscope (Tokyo, Japan), followed by stereological estimation of the numerical density of goblet cells per area [Q_A (goblet cells)], which comprised the division of the total number of goblet cells counted in the test area, except those touching the forbidden line, by the test area (in mm²)[1], obtained with the STEPanizer stereology tool (www.stepanizer.com).

Immunohistochemistry

For immunohistochemistry, slides from the small intestine (ileum) were deparaffinized, and after antigen retrieval (citrate buffer, pH = 6.0, at 60 °C for 20 min), peroxidase and nonspecific binding blocks were added, followed by incubation with a primary antibody against occludin (Invitrogen, 40-4700; Waltham, MA, United States; dilution 1:20) overnight at 4 °C. The antibody was diluted in 1.5% horse serum (Vector Laboratories, CA, United States). The slides were then incubated with a panspecific biotinylated secondary antibody for 10 min followed by incubation with streptavidin and peroxidase for 5 min. The sections were stained with DAB for 5 min (Vectastain Universal Quick HRP Kit, peroxidase, PK-7800, Vector Laboratories). The slides were counterstained with hematoxylin and mounted with Entellan (Merck, Darmstadt, Germany).

Transmission electron microscopy

Cecum fragments (1 mm³, *n* = 3 per group), fixed with 2.5% glutaraldehyde in 0.1 M cacodylate buffer (pH = 7.2) and postfixed with 1% osmium tetroxide, were dehydrated in acetone and added to epoxy resin (48 h at 60/70 °C). Ultrathin sections (60-80 nm) contrasted with 5% uranyl acetate and 2% lead citrate were observed under a transmission electron microscope (FEI, Oregon, United States) at the National Institute of Biochemistry and Bioimaging Science and Technology (CENABIO - UFRJ).

Real-time reverse transcriptase-polymerase chain reaction

Total RNA was extracted from 70 mg of ileum tissue using 700 μL of TRIzol (Invitrogen, CA, United States). Spectrometry and Nanovue equipment (GE Life Sciences) were used to determine the RNA concentration, and cDNA was synthesized using oligo(dT) and Superscript III reverse transcriptase (Invitrogen, CA, United States). *Gapdh* was used as the endogenous control[16].

The efficiencies of the target gene and endogenous control were approximately equal and were calculated from a cDNA dilution series. Polymerase chain reaction (PCR) was performed as follows: Predenaturation and polymerase activation (4 min at 95 °C) with 40 cycles of 95 °C for 10 s and 60 °C for 15 s, followed by melting (60-95 °C with a heating rate of 0.1 °C/s). The cDNA was replaced with deionized water for the negative control. The relative mRNA expression ratio was calculated by the Equation $2^{-\Delta\Delta Ct}$, where -ΔCT represents the difference between the number of cycles of the target genes and the endogenous control. The nomenclature of the genes followed international standards, with the first letter in capital letters and italics. The primers used were generated using Primer3 online software (*Mucin2* - forward: GTAGTTTCCGTTGGAACAGTGAA, reverse: ATGCCCACCTCCTCAAAGAC; and *Gapdh* - forward: CATCACTGC-

CACCCAGAAGACTG, reverse: ATGCCAGTGAGCTTCCCGTTCAG).

16S rRNA gene amplification by qPCR

The feces found in the cecum were used to extract microbial DNA using a commercial kit (QIAamp Fast DNA Stool Mini Kit, Qiagen). Qubit (Life Technologies) and horizontal electrophoresis (1% agarose gel) were used for DNA quantification, and purity and concentration determination. The relative abundance of the main phyla found in the fecal microbiota (*Bacteroidetes*, *Firmicutes*, *Actinobacteria*, and *Proteobacteria*) was assessed *via* real-time quantitative PCR assays by detecting 16S rRNA genes (indicators are listed in Table 1). The abundance of different phyla was normalized to the ΔΔ Ct value of the total amount of bacteria in the sample[17].

Data analysis

The data are presented as the mean and SD. Differences between the groups were tested by the Brown-Forsythe and Welch one-way ANOVA and Dunnett T3 *post hoc* test (GraphPad Prism version 10.1.2 for Windows, GraphPad Software, Boston, MA, United States). $P < 0.05$ was considered to indicate statistical significance.

RESULTS

HFD causes overweight and gut dysbiosis without altering food intake

The four groups started the experiment on mice with similar body masses. At the end of the study, the HF groups were heavier than their counterparts (HF10: +15% *vs* C10; HF16: +22% *vs* C16; Figure 1A). Moreover, compared to HF10 individuals, HF16 individuals were overweight (+6%, Figure 1A). Food intake (in grams) was similar throughout the experiment, irrespective of the diet (C: 2.96 ± 0.08, HF10: 3.00 ± 0.04, C16: 3.01 ± 0.03, and HF16: 3.08 ± 0.04). However, the HF groups had greater energy intake than the C groups (HF10: +33% *vs* C10; HF16: +34% *vs* C16; Figure 1B), which was expected due to the high energy density of the HFD.

Gut dysbiosis occurred in the HFD-fed groups (Figure 1C). Both the HF10 and HF16 groups presented an increased *Firmicutes* proportion concomitant with decreased *Bacteroidetes*, confirming that overweight augments the *Firmicutes*/ *Bacteroidetes* ratio. Notably, the HFD promoted a progressive decrease in the abundance of *Proteobacteria* and *Actinobacteria*. Compared with the HF10 diet, the HF16 diet was associated with a lower proportion of *Proteobacteria* (-83%) and *Actinobacteria* (-76%).

HFD results in time-dependent structural modifications and protection of the intestinal barrier, and induces endotoxemia

High saturated fat intake provoked a time-dependent alteration in the distribution of cecal mucosal cells, as revealed by the reaction of the cells to alcian blue and PAS. Figure 2A shows more goblet cells (stained in blue) in the cecum of the HF10 group than in the cecum of the C10 group. Conversely, the progressive intake of the HFD decreased the Q_A (goblet cells) in the apical region of the crypts in the HF16 group, implying a reduction in mucus production compared to that in the age-matched group. Gut stereology confirmed these observations with the Q_A (goblet cells) results, which were greater in the HF10 group than in the C10 group (+23%), while the HF16 group presented a decrease in Q_A (goblet cells) compared to that in the C16 group (-16%, Figure 2B). The decrease in Q_A (goblet cells) was time-dependent for both diets: C16 and HF16 produced lower Q_A (goblet cells) of the intestine than C10 (-33%) and HF10 (-54%). Consistent with the stereology, the HF10 group presented 55% greater intestinal *Mucin 2* gene expression than the C10 group. On the other hand, the HF16 group did not differ from the C16 group (Figure 2C).

The modifications in the structure and protection of the intestinal barrier in the HF groups caused a marked increase in the plasma concentrations of LPS (HF10: +25% *vs* C10; HF16: +40% *vs* C16; Figure 2D), characterizing endotoxemia. In agreement with the previous results, immunohistochemistry staining for occludin revealed positive reactions in the C10, HF10, and C16 groups, suggesting progressive damage to TJs due to HFD feeding, as HF16 cells showed negative immunoreactions for occludin (Figure 3A).

HFD causes time-dependent damage to the intestinal ultrastructure

Analysis of the intestinal ultrastructure (Figure 3B) revealed that the C10 group had microvilli on the apical surface of the absorptive IEC, in addition to an active mucus layer, numerous mitochondria, and integrity of the cellular membrane. The C16 group also exhibited preservation of the intestinal ultrastructure, as indicated by the presence of intact TJs harboring two consecutive IECs. In contrast, the HF10 group exhibited lipid inclusions inside the IECs parallel to thickened and irregular microvilli, implying damage to cell function. In agreement with previous findings, the HF16 group exhibited a completely disarranged ultrastructure, almost no mitochondria, no microvilli, and permeable TJs.

DISCUSSION

In recent decades, the prevalence of overweight and obesity in developed and developing countries has been increasing due to changes in dietary patterns. Contemporary dietary habits include high energy intake, in forms such as saturated fats and added sugars, and reduced fiber, fruit, and vegetable intake. Therefore, nutritional habits associated with a

Table 1 Primers used for determination of the phylum or class of microorganisms of the gut microbiota

Phylum or class	Forward primer	Reverse primer
Actinobacteria	5'-TACGGCCGCAAGGCTA-3'	5'-TCRTCCCCACCTTCCTCCG-3'
Bacteroidetes	5'-CRAACAGGATTAGATACCCT-3'	5'-GGTAAGGTTCCTCGCGTAT-3'
Class-γ-proteobacteria	5'-TCGTCAGCTCGTGTYGTGA-3'	5'-CGTAAGGGCCATGATG-3'
Eubacteria (all bacteria)	5'-ACTCCTACGGGAGGCAGAGT-3'	5'-ATTACCGCGGCTGCTGGC-3'
Firmicutes	5'-TGAAACTYAAAGGAATTGACG-3'	5'-ACCATGCACCACCTGTC-3'
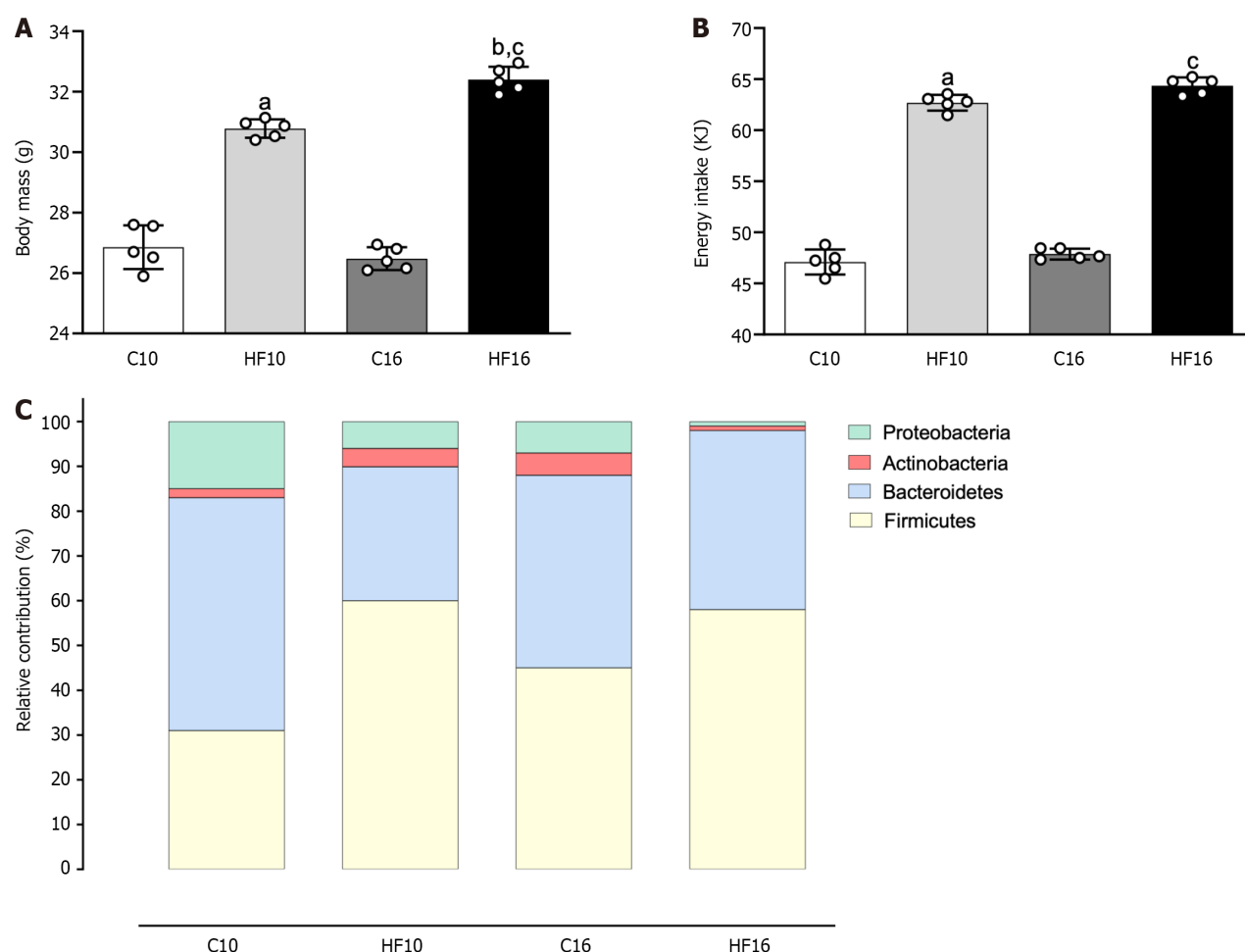
Figure 1 Body mass, energy intake, and phylogenetic microbiota distribution. A: Body mass; B: Energy intake; C: Phylogenetic microbiota distribution. Brown-Forsythe and Welch one-way ANOVA and Dunnett T3 *post hoc* test were used (mean ± SD, *n* = 5). [a]$P < 0.01$, compared with control; [b]$P < 0.01$, compared with high-fat diet for 10 wk; [c]$P < 0.01$ compared with control diet for 16 wk. C10: Control diet for 10 wk; C16: Control diet for 16 wk; HF10: High-fat diet for 10 wk; HF16: High-fat diet for 16 wk.

sedentary lifestyle are strongly related to the genesis and progression of metabolic diseases[18].

The data from this study showed that excessive intake of saturated fatty acids caused increased body mass in C57BL/6 mice fed an HFD for 10 or 16 wk. Chronic high saturated fat intake yields low-grade inflammation and impairs cellular carbohydrate and lipid metabolism, causing weight gain owing to the high energy density of saturated fat[19]. In contrast, there was no difference in food intake between the experimental groups, implying that the metabolic alterations could stem from excessive energy intake from saturated fatty acids.

Lipotoxicity provokes alterations in the intestinal barrier and gut microbiota, favoring obesity[6]. The human intestine is colonized by up to 100 trillion microorganisms, which is approximately ten times the number of human cells. Many factors influence the microbiota composition over the course of a person's life, mainly diet, route of birth delivery, and the use of medications, especially antibiotics[20].

Out of more than 50 described phyla, four predominate: *Firmicutes*, *Bacteroidetes*, *Actinobacteria*, and *Proteobacteria*[21]. Recent studies have shown that an HFD increases the *Firmicutes* and *Proteobacteria* proportions concomitant with decreased *Bacteroidetes*. The abundance of *Proteobacteria* usually increases in obese individuals, and *Proteobacteria* is
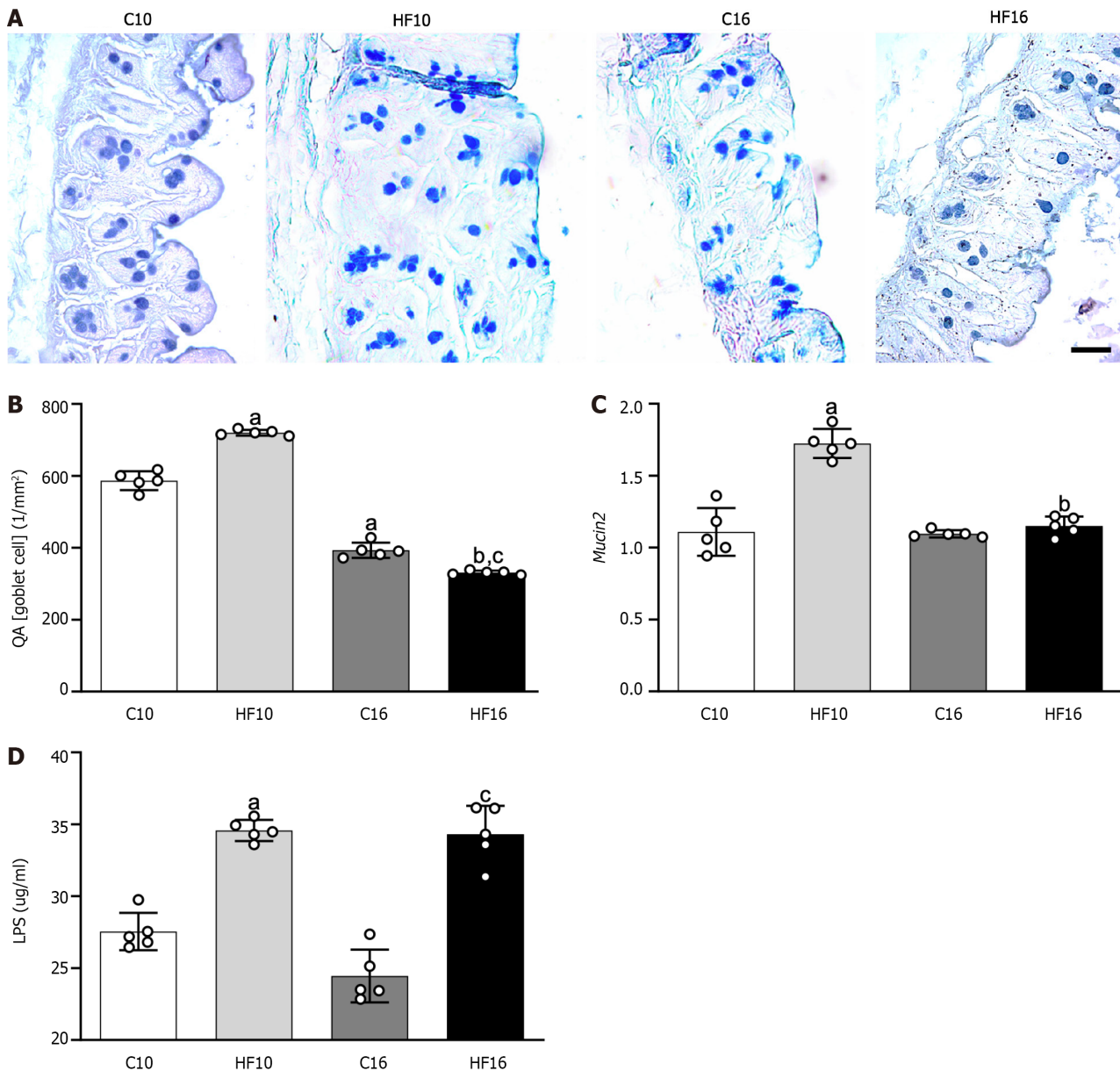
Figure 2 Staining of goblet cells with alcian blue, Q$_A$ (goblet cells), relative *Mucin2* mRNA expression, and plasma lipopolysaccharide concentrations. A: Large intestine tissue stained with alcian blue and periodic acid-Schiff (PAS), revealing that the goblet cells were stained blue; B: Numerical density of goblet cells per area [Q$_A$ (goblet cells)]. Alcian blue and PAS stained glycoproteins produced by goblet cells (scale bar = 40 μm) were markedly increased in the high-fat diet for 10 wk group according to stereology [Q$_A$ (goblet cells)]. ; C: Relative *Mucin2* mRNA expression in different groups; D: Plasma lipopolysaccharide concentrations in different groups. Brown-Forsythe and Welch one-way ANOVA and Dunnett T3 *post hoc* test were used (mean ± SD, *n* = 5). [a]$P < 0.01$, compared with control; [b]$P < 0.01$, compared with high-fat diet for 10 wk; [c]$P < 0.01$ compared with control diet for 16 wk. C10: Control diet for 10 wk; C16: Control diet for 16 wk; HF10: High-fat diet for 10 wk; HF16: High-fat diet for 16 wk; LPS: Lipopolysaccharide.

emerging as a possible marker of microbiota variability and metabolic constraints[22]. However, in mice, the proportion of *Proteobacteria* increases more in response to high-carbohydrate conditions than to HF conditions[1,23]. Notably, both the HF10 and HF16 populations exhibited a marked decrease in *Actinobacteria*, which strongly suggested impaired gut homeostasis. *Bifidobacteria*, a class of *Actinobacteria*, are widely used as probiotics to treat many diseases[24]. In addition to gut dysbiosis, the increase in plasma LPS in the HF10 and HF16 groups suggested intestinal paracellular permeability changes, characterizing metabolic endotoxemia[23].

TJ proteins are responsible for sealing the intestinal mucosa and maintaining barrier function by regulating the permeability of the intestinal mucosa[25]. The role of occludin in TJs seems to encompass the macromolecular permeability barrier, although this phenomenon is still under debate[9]. Our investigation revealed that occludin expression decreased in a time-dependent manner in HFD-fed mice, with a negative immunoreaction in the HF16 group. When large molecules are abnormally translocated from the lumen to the villi, these molecules are absorbed; this process is called leaky gut, which was presented by HF10 and HF16 mice, in agreement with the literature[26].

Within this context, altered intestinal permeability is highly detrimental, as it loses its ability to block the systemic entry of harmful agents, whether food-derived microorganisms or antigens. An increase in the endotoxin LPS in systemic
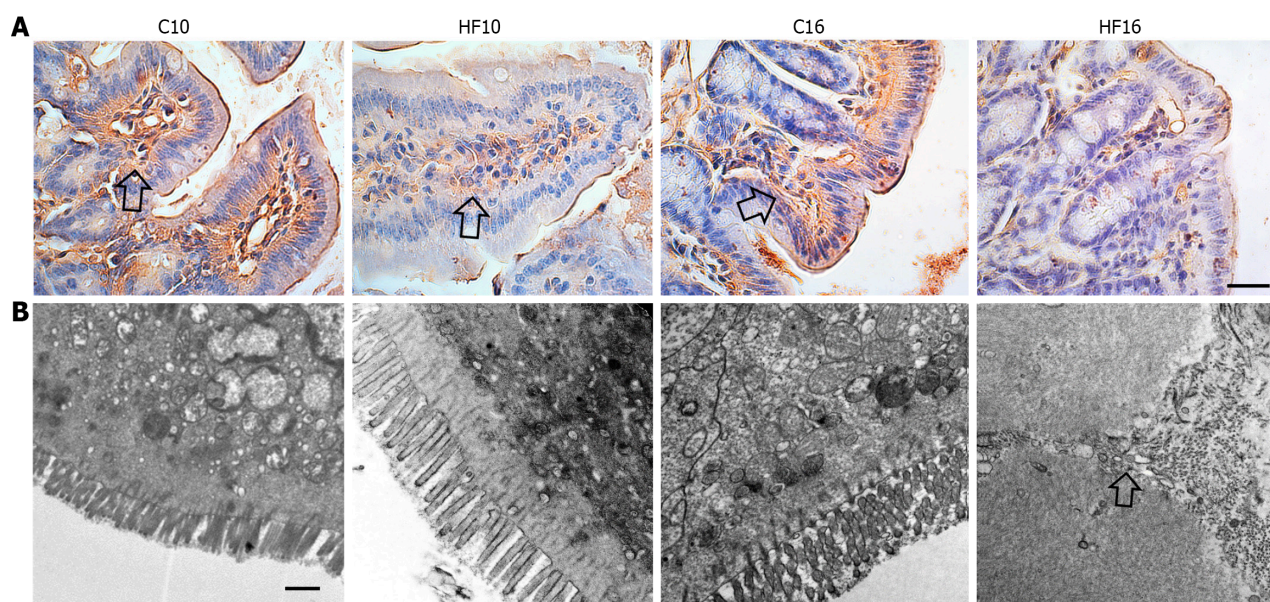
Figure 3 Immunohistochemical staining for occludin in the ileum and transmission electron microscopy of the ileum. A: Occludin immunostaining is shown in light brown (open arrow) and was decreased in a time-dependent manner in the high-fat (HF)-fed groups. B: Transmission electron microscopy images showing normal ileal ultrastructures in the control diet for 10 wk and control diet for 16 wk groups, with preserved tight junctions (asterisk). In contrast, the HF diet for 10 wk and HF diet for 16 wk groups exhibited disrupted tight junctions (open arrow) in addition to a damaged ultrastructure. C10: Control diet for 10 wk; C16: Control diet for 16 wk; HF10: High-fat diet for 10 wk; HF16: High-fat diet for 16 wk.

circulation culminates in the release of proinflammatory cytokines, triggering tissue damage in several systems[27].

Goblet cells are ubiquitously present in the intestinal epithelium and secrete vesicles composed mainly of mucin that are found between enterocytes. Its mucus-producing characteristic confers the ability to lubricate and protect the intestinal epithelium[28]. The histological analysis of this study revealed the presence of numerous goblet cells in the HF10 group, suggesting an attempt to compensate for the alterations caused by bacterial products and toxins by stimulating the thickening of the mucus layer of the intestinal epithelium in response to tissue damage, such as LPS, which also had high plasma levels in this group[13]. On the other hand, the progression of dietary intake in the HF16 group caused a reduction in the Q_A (goblet cells). This time-dependent reduction in the Q_A (goblet cells) was related to *Mucin2* gene expression and was consistent with the adverse ultrastructural remodeling observed in the HF16 group.

Secretory mucins, such as Mucin2, which are present in the small and large intestines, are the chief mucins synthesized and secreted by goblet cells. Mucin2 secretion is stimulated by a wide range of bioactive factors, including microbial products, toxins, and inflammatory cytokines, which are reportedly involved in the up- or downregulation of *Mucin2* transcription. The microbiota and microbial products can modulate the synthesis and secretion of Mucin2, either through several signaling cascades or through bioactive factors generated by epithelial and lamina propria cells[29]. The Q_A (goblet cells) indirectly reflects the ability to secrete Mucin2. Thus, *Mucin2* gene expression followed that of the Q_A (goblet cells), indicating time-dependent damage caused by the HFD to the mucus layer of the intestinal mucosa[12].

A dysfunctional intestinal mucus system and altered goblet cell profile are associated with maturity and inflammatory conditions in mice, resulting in a thin mucus layer and increased vulnerability to infections[30]. A previous study revealed the occurrence of an infection process that progresses through the dysregulation of the microvillus and the presence of cavities on the epithelial surface[31]. In this sense, transmission electron microscopy revealed that HFD intake led to time-dependent changes in the mucous layer and impairment of microvilli, a reduction in mitochondria within the EICs, and damaged TJs in the HF16 group, consistent with the negative occludin immunostaining in the HF16 group, metabolic endotoxemia, and aggravation of obesity from 10 to 16 wk of HFD feeding. Figure 4 summarizes our main findings.

CONCLUSION

In conclusion, chronic HF intake causes overweight, gut dysbiosis, and morphological and functional alterations in the intestinal barrier after 10 or 16 wk. The increased plasma LPS concentrations in the HF groups occurred after progressive damage to mucus-producing cells and occludin (TJ protein) expression. Our results provided original evidence of enhanced Q_A (goblet cells) in the HF10 group as compensatory hyperplasia triggered by lipotoxicity followed by a reduced Q_A (goblet cells) in the HF16 group with maximization of ultrastructural intestinal damage and obesity. The present results highlight the exacerbation of obesity-driven intestinal alterations from 10 to 16 wk of the dietary protocol, suggesting new targets for further studies aimed at obesity management.
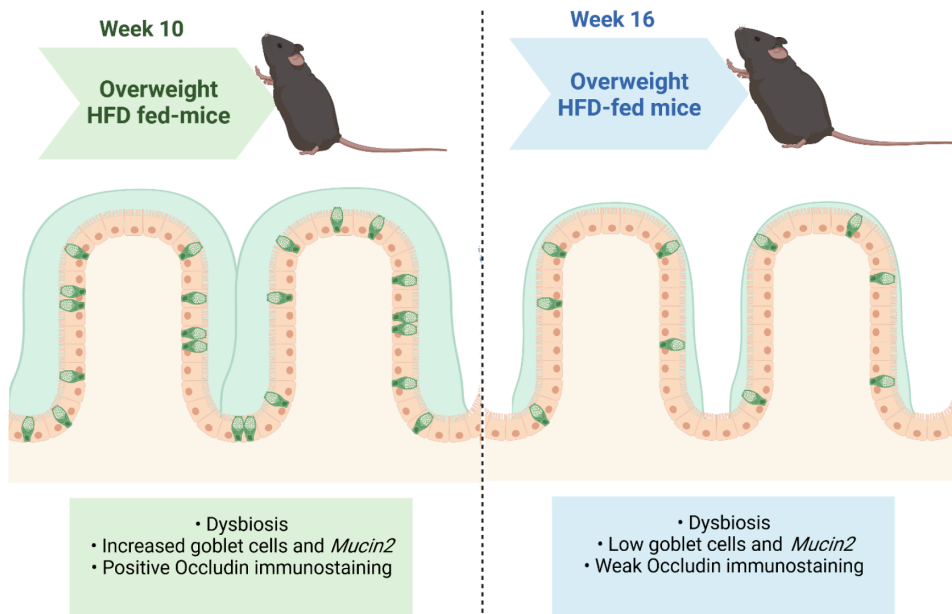
Figure 4 Summary of the main results. The animals fed the high-fat diet for 10 wk (HF10) had overweight, increased goblet cell numerical density, and *Mucin2* expression as a compensatory mechanism to prevent injury from the HFD. However, after 16 wk, HFD-fed mice remained overweight and had a greater body mass than the HF10 group but had a decreased goblet cell number and *Mucin2* expression. Therefore, HF16 mice exhibited a completely disarranged intestinal ultrastructure, with damaged tight junctions and negative occludin immunostaining. Created with Biorender (www.biorender.com). HFD: High-fat diet.

ARTICLE HIGHLIGHTS

Research background

There is great interest in the scientific community in the role of gut dysbiosis in obesity and metabolic impairments. However, there is little evidence in the literature on the progressive impact of a high-fat diet (HFD) on mouse intestinal barrier structure and microbiota composition.

Research motivation

Recently, different dietary models and durations of diet administration have yielded controversial results regarding the Q_A (goblet cells), mucus layer, and microbiota composition in mice with diet-induced obesity. Considering the importance of understanding the progressive changes in intestinal structure and microbiota composition that occur during obesity onset, we examined these changes after 10 or 16 wk of HFD feeding to establish tools to characterize obesity-related intestinal impairments.

Research objectives

We further studied the chronic effects (at 10 and 16 wk) of an HFD (with 50% energy as fat) on the phylogenetic gut microbiota distribution and intestinal barrier structure and protection in C57BL/6 mice. The study considered the mouse model, diet composition, and duration of intervention that were most prevalent in the literature.

Research methods

Mice were fed *ad libitum*, and food intake and body mass gain were monitored during the experiment. Intestinal samples were subjected to light and electron microscopy, and plasma lipopolysaccharide concentrations were determined through ELISA. After 16S rRNA gene amplification by qPCR was performed on the frozen cecal feces to determine the phylogenetic microbiota distribution, the ileum samples were subjected to qPCR analysis for *Occludin* expression.

Research results

Our results confirmed that body mass increased gradually with HFD feeding without altering food intake. Dysbiosis in the HFD model involved an increase in *Firmicutes* and a decrease in *Bacteroidetes* concomitant with an increase in plasma lipopolysaccharide concentrations, so-called endotoxemia. The original findings were compensatory goblet cell hyperplasia and increased *Mucin2* expression in the tenth week, followed by a drastic reduction in both parameters after 16 wk of HFD feeding. These structural alterations were consistent with the progressive damage to the intestinal ultrastructure in obese mice.

Research conclusions

Chronic HFD intake causes gut dysbiosis and endotoxemia, with time-dependent overweight, and morphological and functional alterations of the intestinal barrier after 10 or 16 wk. We identified Q_A (goblet cells) and mucin expression as

viable tools to address the progressive damage caused by obesity in the intestine.

Research perspectives

The evaluation of QA (goblet cells), functionality, and ultrastructure has led to the identification of potential targets for addressing the impact of excessive saturated fatty acid intake on the intestine.

ACKNOWLEDGEMENTS

The authors thank Aline Penna and Andrea Bertoldo for their technical assistance and "Unidade de Microscopia Multiusuário Padrón-Lins (UNIMICRO)" for obtaining and preparing the transmission electron microscopy grids.

FOOTNOTES

REFERENCES

1　**Silva-Veiga FM**, Miranda CS, Vasques-Monteiro IML, Souza-Tavares H, Martins FF, Daleprane JB, Souza-Mello V. Peroxisome proliferator-activated receptor-alpha activation and dipeptidyl peptidase-4 inhibition target dysbiosis to treat fatty liver in obese mice. *World J Gastroenterol* 2022; **28**: 1814-1829 [PMID: 35633911 DOI: 10.3748/wjg.v28.i17.1814]

2　**Zhou Y**, Li C, Wang X, Deng P, He W, Zheng H, Zhao L, Gao H. Integration of FGF21 Signaling and Metabolomics in High-Fat Diet-Induced Obesity. *J Proteome Res* 2021; **20**: 3900-3912 [PMID: 34237942 DOI: 10.1021/acs.jproteome.1c00197]

3　**Zhu Y**, Shi C, Niu Q, Wang J, Zhu W. Dynamic changes in morphology, gene expression and microbiome in the jejunum of compensatory-growth rats induced by protein restriction. *Microb Biotechnol* 2018; **11**: 734-746 [PMID: 29633535 DOI: 10.1111/1751-7915.13266]

4　**Cani PD**, Bibiloni R, Knauf C, Waget A, Neyrinck AM, Delzenne NM, Burcelin R. Changes in gut microbiota control metabolic endotoxemia-induced inflammation in high-fat diet-induced obesity and diabetes in mice. *Diabetes* 2008; **57**: 1470-1481 [PMID: 18305141 DOI: 10.2337/db07-1403]

5　**Hersoug LG**, Møller P, Loft S. Role of microbiota-derived lipopolysaccharide in adipose tissue inflammation, adipocyte size and pyroptosis during obesity. *Nutr Res Rev* 2018; **31**: 153-163 [PMID: 29362018 DOI: 10.1017/S0954422417000269]

6　**Silva-Veiga FM**, Miranda CS, Martins FF, Daleprane JB, Mandarim-de-Lacerda CA, Souza-Mello V. Gut-liver axis modulation in fructose-fed mice: a role for PPAR-alpha and linagliptin. *J Endocrinol* 2020; **247**: 11-24 [PMID: 32698143 DOI: 10.1530/JOE-20-0139]

7　**Nascimento JC**, Matheus VA, Oliveira RB, Tada SFS, Collares-Buzato CB. High-Fat Diet Induces Disruption of the Tight Junction-Mediated Paracellular Barrier in the Proximal Small Intestine Before the Onset of Type 2 Diabetes and Endotoxemia. *Dig Dis Sci* 2021; **66**: 3359-3374 [PMID: 33104937 DOI: 10.1007/s10620-020-06664-x]

8 **Turner JR**. Intestinal mucosal barrier function in health and disease. *Nat Rev Immunol* 2009; **9**: 799-809 [PMID: 19855405 DOI: 10.1038/nri2653]

9 **Otani T**, Furuse M. Tight Junction Structure and Function Revisited. *Trends Cell Biol* 2020; **30**: 805-817 [PMID: 32891490 DOI: 10.1016/j.tcb.2020.08.004]

10 **Verediano TA**, Sant'Ana C, Grancieri M, Tako E, Paes MCD, Martino HSD. Black corn (Zea mays L.) flour has the potential to improve the gut microbiota composition and goblet cell proliferation in mice fed a high-fat diet. *Nutr Res* 2022; **108**: 60-72 [PMID: 36403535 DOI: 10.1016/j.nutres.2022.10.005]

11 **Fu J**, Wei B, Wen T, Johansson ME, Liu X, Bradford E, Thomsson KA, McGee S, Mansour L, Tong M, McDaniel JM, Sferra TJ, Turner JR, Chen H, Hansson GC, Braun J, Xia L. Loss of intestinal core 1-derived O-glycans causes spontaneous colitis in mice. *J Clin Invest* 2011; **121**: 1657-1666 [PMID: 21383503 DOI: 10.1172/JCI45538]

12 **Odenwald MA**, Turner JR. The intestinal epithelial barrier: a therapeutic target? *Nat Rev Gastroenterol Hepatol* 2017; **14**: 9-21 [PMID: 27848962 DOI: 10.1038/nrgastro.2016.169]

13 **Benoit B**, Laugerette F, Plaisancié P, Géloën A, Bodennec J, Estienne M, Pineau G, Bernalier-Donadille A, Vidal H, Michalski MC. Increasing fat content from 20 to 45 wt% in a complex diet induces lower endotoxemia in parallel with an increased number of intestinal goblet cells in mice. *Nutr Res* 2015; **35**: 346-356 [PMID: 25687164 DOI: 10.1016/j.nutres.2015.01.005]

14 **Valdes J**, Gagné-Sansfaçon J, Reyes V, Armas A, Marrero G, Moyo-Muamba M, Ramanathan S, Perreault N, Ilangumaran S, Rivard N, Fortier LC, Menendez A. Defects in the expression of colonic host defense factors associate with barrier dysfunction induced by a high-fat/high-cholesterol diet. *Anat Rec (Hoboken)* 2023; **306**: 1165-1183 [PMID: 36196983 DOI: 10.1002/ar.25083]

15 **Reeves PG**, Nielsen FH, Fahey GC Jr. AIN-93 purified diets for laboratory rodents: final report of the American Institute of Nutrition ad hoc writing committee on the reformulation of the AIN-76A rodent diet. *J Nutr* 1993; **123**: 1939-1951 [PMID: 8229312 DOI: 10.1093/jn/123.11.1939]

16 **Miranda CS**, Silva-Veiga FM, Fernandes-da-Silva A, Guimarães Pereira VR, Martins BC, Daleprane JB, Martins FF, Souza-Mello V. Peroxisome proliferator-activated receptors-alpha and gamma synergism modulate the gut-adipose tissue axis and mitigate obesity. *Mol Cell Endocrinol* 2023; **562**: 111839 [PMID: 36581062 DOI: 10.1016/j.mce.2022.111839]

17 **Livak KJ**, Schmittgen TD. Analysis of relative gene expression data using real-time quantitative PCR and the 2(-Delta Delta C(T)) Method. *Methods* 2001; **25**: 402-408 [PMID: 11846609 DOI: 10.1006/meth.2001.1262]

18 **Lambertz J**, Weiskirchen S, Landert S, Weiskirchen R. Fructose: A Dietary Sugar in Crosstalk with Microbiota Contributing to the Development and Progression of Non-Alcoholic Liver Disease. *Front Immunol* 2017; **8**: 1159 [PMID: 28970836 DOI: 10.3389/fimmu.2017.01159]

19 **Rangel-Azevedo C**, Santana-Oliveira DA, Miranda CS, Martins FF, Mandarim-de-Lacerda CA, Souza-Mello V. Progressive brown adipocyte dysfunction: Whitening and impaired nonshivering thermogenesis as long-term obesity complications. *J Nutr Biochem* 2022; **105**: 109002 [PMID: 35346828 DOI: 10.1016/j.jnutbio.2022.109002]

20 **Hasan N**, Yang H. Factors affecting the composition of the gut microbiota, and its modulation. *PeerJ* 2019; **7**: e7502 [PMID: 31440436 DOI: 10.7717/peerj.7502]

21 **Magne F**, Gotteland M, Gauthier L, Zazueta A, Pesoa S, Navarrete P, Balamurugan R. The Firmicutes/Bacteroidetes Ratio: A Relevant Marker of Gut Dysbiosis in Obese Patients? *Nutrients* 2020; **12** [PMID: 32438689 DOI: 10.3390/nu12051474]

22 **Rizzatti G**, Lopetuso LR, Gibiino G, Binda C, Gasbarrini A. Proteobacteria: A Common Factor in Human Diseases. *Biomed Res Int* 2017; **2017**: 9351507 [PMID: 29230419 DOI: 10.1155/2017/9351507]

23 **Vasques-Monteiro IML**, Silva-Veiga FM, Miranda CS, de Andrade Gonçalves ÉCB, Daleprane JB, Souza-Mello V. A rise in Proteobacteria is an indicator of gut-liver axis-mediated nonalcoholic fatty liver disease in high-fructose-fed adult mice. *Nutr Res* 2021; **91**: 26-35 [PMID: 34130208 DOI: 10.1016/j.nutres.2021.04.008]

24 **Binda C**, Lopetuso LR, Rizzatti G, Gibiino G, Cennamo V, Gasbarrini A. Actinobacteria: A relevant minority for the maintenance of gut homeostasis. *Dig Liver Dis* 2018; **50**: 421-428 [PMID: 29567414 DOI: 10.1016/j.dld.2018.02.012]

25 **Nakanishi T**, Fukui H, Wang X, Nishiumi S, Yokota H, Makizaki Y, Tanaka Y, Ohno H, Tomita T, Oshima T, Miwa H. Effect of a High-Fat Diet on the Small-Intestinal Environment and Mucosal Integrity in the Gut-Liver Axis. *Cells* 2021; **10** [PMID: 34831391 DOI: 10.3390/cells10113168]

26 **Usuda H**, Okamoto T, Wada K. Leaky Gut: Effect of Dietary Fiber and Fats on Microbiome and Intestinal Barrier. *Int J Mol Sci* 2021; **22** [PMID: 34299233 DOI: 10.3390/ijms22147613]

27 **Schoeler M**, Caesar R. Dietary lipids, gut microbiota and lipid metabolism. *Rev Endocr Metab Disord* 2019; **20**: 461-472 [PMID: 31707624 DOI: 10.1007/s11154-019-09512-0]

28 **Lueschow SR**, McElroy SJ. The Paneth Cell: The Curator and Defender of the Immature Small Intestine. *Front Immunol* 2020; **11**: 587 [PMID: 32308658 DOI: 10.3389/fimmu.2020.00587]

29 **Birchenough GM**, Johansson ME, Gustafsson JK, Bergström JH, Hansson GC. New developments in goblet cell mucus secretion and function. *Mucosal Immunol* 2015; **8**: 712-719 [PMID: 25872481 DOI: 10.1038/mi.2015.32]

30 **Gustafsson JK**, Johansson MEV. The role of goblet cells and mucus in intestinal homeostasis. *Nat Rev Gastroenterol Hepatol* 2022; **19**: 785-803 [PMID: 36097076 DOI: 10.1038/s41575-022-00675-x]

31 **Ritchie JM**, Rui H, Zhou X, Iida T, Kodoma T, Ito S, Davis BM, Bronson RT, Waldor MK. Inflammation and disintegration of intestinal villi in an experimental model for Vibrio parahaemolyticus-induced diarrhea. *PLoS Pathog* 2012; **8**: e1002593 [PMID: 22438811 DOI: 10.1371/journal.ppat.1002593]